Dominant instability mechanism of VSI connecting to a very weak grid

Chuanyue Li, *Member, IEEE,* Sheng Wang, *Member, IEEE,* Frederic Colas, Jun Liang, *Senior Member, IEEE*

Abstract—In this paper, it is identified that unstable weak grid connection of voltage source inverters (VSIs) is dominantly caused by the current control. In particular, it is found the proportional gain k_p of conventional PI controller cannot balance the grid voltage impact and damping capability especially when a very weak grid with short circuit ratio (SCR) < 1.3 is connected. This issue is solved in this paper by simply restructuring the PI controller as an IP controller for current control. This IP controller will not change the tuning method of current control and make this VSI indeed connect to a very weak grid with rated power injection.

I. Introduction

VOLTAGE source inverters (VSIs) located far from the AC grid risk instability due to weak-grid connection, which is defined as SCR<3 [1]. Oscillations caused by VSIs connecting to weak grids have been observed in many regional grids, such as Texas 4 Hz oscillations, West China 30 Hz oscillations and UK 8-9 Hz oscillations [2]. This oscillation can further induce the torsional interaction with synchronization generators [3]. Interaction between VSI's phase-locked loop (PLL) based vector control and high grid impedance causes this instability. This VSI control is presented in Fig. 1. Analysis on its mechanism of instability are extensively conducted and the following guidelines have been drawn: high grid inductance raises the risk of instability [4]; slowing control system (equivalently reducing control bandwidth) including PLL [5] and vector control [6] helps to stabilize the weak-grid connection; in outer loop, faster ac voltage control over power control [7] helps the VSI stabilization.

However, when connecting to a very weak grid with SCR < 1.3, extensive tuning attempts using the guidelines above still cannot stabilize this VSI [8].

For connecting VSIs to such very weak grids, additional compensation control blocks have been proposed. These control blocks can be embedded within either the outer loop or the PLL. With the outer loop, additional control blocks can be added to decouple the voltage and power [9] or suppress the voltage impact on power control [10]. With the PLL, virtually reducing grid impedance [11] for enhancing voltage stiffness at the tracking point also enables rated power injection to a very weak grid.

Despite significant contributions have been made to mitigate the instability issues, the dominant cause of this very-weak-grid instability is yet identified. Also, using additional compensation control blocks significantly increase the control complexity.

To close the gap, in this paper, it is identified the current control dominantly causes instability of the very-weak-grid connection. In particular, it is found k_p tuning of current controller cannot balance between reducing voltage impact on point of common coupling (PCC) and enhancing damping capability. Based on this finding, without any compensation
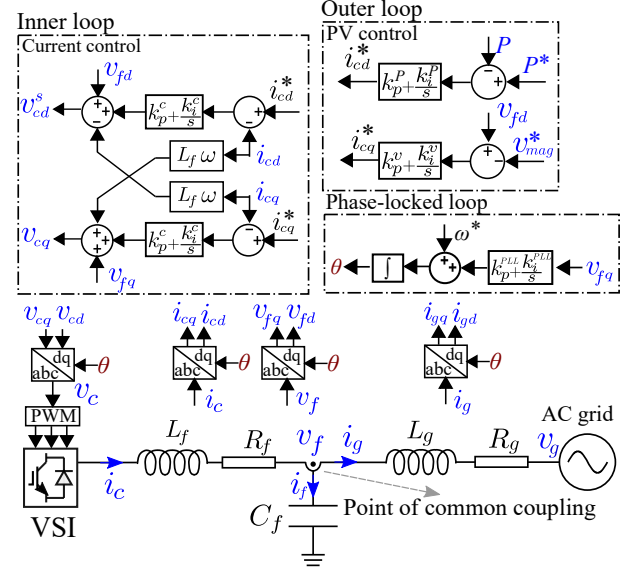

Fig. 1. A PLL-based VSI connecting to the AC grid.

control, a solution is proposed by simply restructuring the PI controller as an IP controller to allow VSIs connecting to a very weak grid (SCR< 1.3). Finally, a switching model of a two-level VSI is used to validate this solution.

II. Dominant instability mechanism of inverter control

A VSI system using PLL-based vector control is shown in Fig. 1, its parameters are from [6]. The static dq current operation area of a VSI connecting to a very weak grid (SCR=1) is calculated and presented in Fig. 2(a). Firstly, it is found that inverter current injection such as i_{cd} has a significant impact on the voltage at point of common coupling (PCC), which will not happen to a strong grid. For example, at point D in Fig. 2(a), only increasing i_{cd} to 1 p.u. drops v_{fd} to 0.24 p.u., where v_{fd} is the PCC voltage. Secondly, it is found that rated power injection ($i_{cd} = 1$ and $v_{fd} = 1$) of a VSI is still feasible at point C. However, by small-signal stability analysis, this operation point C is unreachable due to instability issue. As shown in Fig. 2(b) this VSI loses stability
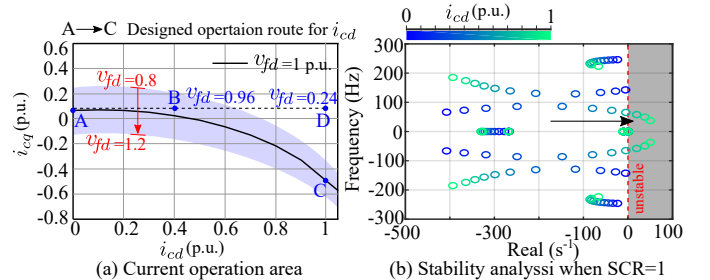

(a) Current operation area   (b) Stability analyssi when SCR=1

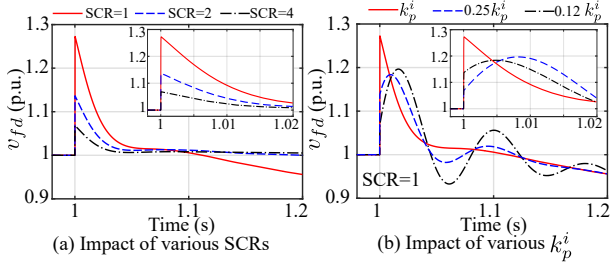Fig. 2. Weak grid impact on static current exchange when SCR=1.

Fig. 3. Voltage fluctuation caused by current control at $\Delta i_{cd}^* = 0.4$ p.u. (Current control: $\zeta^c = 0.707$ $w_n^c = 160$; PLL: $\zeta^{PLL} = 0.707$ $w_n^{PLL} = 11$).

with increasing i_{cd} at constant $v_{fd} = 1$ p.u.. Obviously, this instability is caused by the control system.

As reviewed in Introduction, outer loop or PLL requires additional compensation control blocks to stabilize this VSI with very-weak-grid connection, which reflects that they are not the dominant causes.

When a very weak grid is connected, PCC voltage fluctuation caused by the current control severely increases and significantly disturb the stable grid connection. It is presented below that how the current control dominates this very-weak-grid instability.

The relation between current reference $\mathbf{i}_c^*$ and inverter output current $\mathbf{i}_c$ is given:

$$\Delta\mathbf{i}_c = \frac{k_p^c s + k_i^c}{L_f s^2 + (R_f + k_p^c)s + k_i^c}\Delta\mathbf{i}_c^* \tag{1}$$

where bold $\mathbf{i}$ is a matrix contains dq components $[i_d; i_q]$, k_p^c and k_i^c are the gains of PI controller applied in a current control.

Within low frequency range, C_f is ignored to assume $\mathbf{i}_c = \mathbf{i}_g$. Therefore, $\mathbf{v}_f$ is expressed as:

$$\Delta\mathbf{v}_f = \begin{bmatrix} L_g s + R_g & -\omega_0 L_g \\ \omega_0 L_g & L_g s + R_g \end{bmatrix}\Delta\mathbf{i}_c \tag{2}$$

It is assumed that only i_{cd}^* or i_{cq}^* is regulated at the same time. Therefore, coupling parts $\omega_0 L_g$ of grid impedance are ignored. Substituting $\Delta\mathbf{i}_c$ in (2) with (1) yields:

$$\Delta\mathbf{v}_f = \frac{(k_p^c s + k_i^c)(L_g s + R_g)}{L_f s^2 + (R_f + k_p^c)s + k_i^c}\Delta\mathbf{i}_c^* \tag{3}$$

The relation between PCC voltage and current control is yielded by rearranging (3):

$$\Delta\mathbf{v}_f = (\underbrace{\frac{k_p^c L_g}{L_f}}_{\text{coeff.a.1}} - \underbrace{\frac{k_p^c L_g}{L_f}\frac{(k_p^c + R_f - (k_p^c R_g L_f/k_i^c L_g)s + k_i^c)}{L_f s^2 + (R_f + k_p^c)s + k_i^c}}_{\text{coeff.a.2}}$$
$$+ \underbrace{\frac{k_i^c(L_g s + R_g)}{L_f s^2 + (R_f + k_p^c)s + k_i^c}}_{\text{coeff.b}})\Delta\mathbf{i}_c^* \tag{4}$$

At $t = 0$ s, $(-\text{coeff.a.2} + \text{coeff.b})\Delta\mathbf{i}_c^*$ in (4) is 0, which results in:

$$\Delta\mathbf{v}_f|_{t=0} = \frac{k_p^c L_g}{L_f}\Delta\mathbf{i}_c^* \tag{5}$$

How a current control disturbs the PCC voltage is found below based on (4) (5):

(i) weak grid (high L_g) causes significant voltage surge $\Delta\mathbf{v}_f|_{t=0}$ based on (5)

(ii) reducing k_p^c helps to mitigate this voltage surge

(iii) k_p^c also determines the damping ratio based on (4)'s denominator, reducing k_p^c may induce a significant PCC voltage oscillation.

A conflict appears on k_p^c tuning as described in (ii) and (iii). Although the PCC voltage surge can be mitigated by reducing k_p^c, a new PCC voltage oscillation may be induced by this k_p^c reduction.

A time-domain validation of above findings (i-iii) are implemented via a PLL-based current-controlled VSI. For accurate and clear validation, the average model of VSI is used and capacitor C_f is removed. SCR=1 with $X_{L_g} : R_g = 10 : 1$.

As shown in Fig. 3(a), when t=1 s, $\Delta i_{cd}^* = 0.4$ p.u. is applied, the voltage surge is increasing with the decrement of SCR, where SCR=$1/Z_g$. This trend fits the finding 1). The peak values of Δv_{fd} are calculated as [0.26 0.13 0.065] based on (5) with SCR=1, 2, 4, which also matches the simulation results of Δv_{fd} at 1 s, as shown in Fig. 3(a).

To suppressing this voltage surge, k_p^c is reduced based on (5) and its simulation result is shown in 3(b). It is obvious that k_p^c reduction helps to reduce the voltage surge at 1 s, which proves the finding (ii). However, severe voltage resonance occurs with k_p^c decrement. This low damping performance also fits the finding (iii).

In a sum, weaker grid causes a higher PCC voltage impact of current control. Furthermore, this PCC voltage impact can not be eliminated by the current control when an very weak grid is connected SCR<1.3. It is because a conflict appears on k_p^c tuning based on findings (ii) and (iii), which is that reducing voltage surge will cause low damping capability and vice versa. This is the dominant instability mechanism of VSI connecting to a very weak grid.

III. Solution for the Dominant Instability Mechanism

To solve the above-mentioned issue, the PI controller in current control is restructured as an IP controller, as shown in Fig. 4. The transfer function of current control based on this IP controller is derived below:

$$\Delta\mathbf{i}_c = \frac{k_i^c}{L_f s^2 + (R_f + k_p^c)s + k_i^c}\Delta\mathbf{i}_c^* \tag{6}$$

Comparing to original transfer function (1) of the current control, (6) has the same second order denominator, which means this IP-based current control can still use the same tuning method.
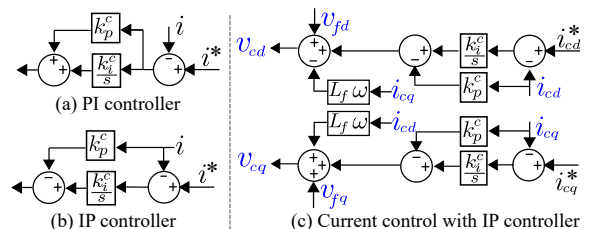

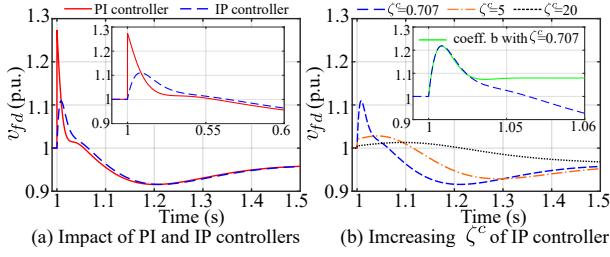Fig. 4. Current control using IP controller.

Fig. 5. Comparison between PI controller and IP controller, and IP controller damping enhancement at $\Delta i_{cd}^* = 0.4$ p.u.. (Current control: $\zeta^c = 0.707$ $w_n^c = 160$; PLL: $\zeta^{PLL} = 0.707$ $w_n^{PLL} = 11$).
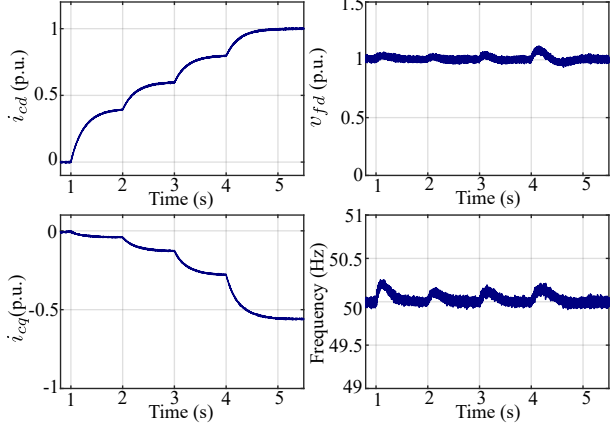

Fig. 6. Starting process of rated power injection at SCR=1 with switching VSI model (Current control: $\zeta^c = 20$ $w_n^c = 160$; PLL: $\zeta^{PLL} = 0.707$ $w_n^{PLL} = 11$).

Based on (6), the relation between PCC voltage and current control is yielded:

$$\Delta \mathbf{v}_f = \underbrace{\frac{k_i^c(L_g s + R_g)}{L_f s^2 + (R_f + k_p^c)s + k_i^c}}_{\text{coeff.b}} \Delta \mathbf{i}_c^* \qquad (7)$$

Thanks to this IP controller, coeff.a.1 and coeff.a.2 in (4) are eliminated. Therefore, the voltage surge caused by PI controller via coeff.a.1 will not be avoided by current control using IP controller. k_p^c tuning only needs to consider the current damping capability.

A. Simulation validation

A simulation result comparing the effectiveness of PI controller and IP controller is shown in Fig. 5(a). Same k_p^c and k_i^c are applied for both PI and IP controllers. After $\Delta i_{fd*} = 0.4$ is applied, it is obvious that the voltage surge (red line) at t=1 s caused by the PI controller will not happen when an IP controller is applied (blue dashed line), which fits the analysis based on (7).

Therefore, the conflict of k_p^c tuning is avoided, because enhancing the damping capability of the current control will not cause the significant voltage surge caused by coeff.a.1.

A validation of (7) is shown in Fig. 5(b)'s small figure, it is found that the voltage overshoot appears in simulation result matches the (7). Therefore, damping this voltage overshoot based on (7) is effective.
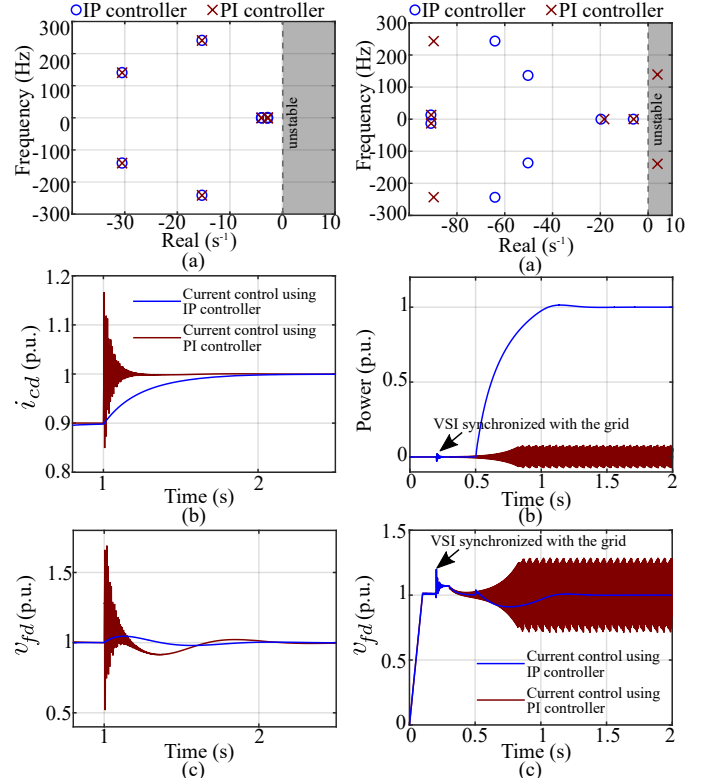

Fig. 7. Small-signal stability analysis for PLL-based current control

Fig. 8. Small-signal stability analysis for PLL-based PV control

The simulation result of enhancing the damping capability of current controller is also shown in Fig. 5(b). $\zeta^c = 0.707$ of the current control is not enough to damp the voltage overshoot (blue dashed line), this is because that a weak grid (high inductance) will enlarge the voltage overshoot via the zero in (7). Therefore, high damping ratios are applied for current control, and this voltage overshoot is well damped at $\zeta^c = 20$.

Finally, based on the analysis above, a switching model of a two-level converter with LC filter is used to validate the PLL-based current controller using IP controller. A starting process of the rated power injection at SCR=1 $X_{L_g} : R_g = 10 : 1$ is presented in Fig. 6. The regulation of i_{cd}^* and i_{cq}^* follows the route in Fig. 2(a) from point A to point C. The results prove that a current control using IP controllers enable the VSI connect to a very weak grid at SCR=1 with rated power injection.

A very weak grid tested above is the worst case for VSI integration, the proposed solution is also validated to be suitable for connecting VSIs to grid with SCR> 1.3.

B. Small-signal stability assessment

The small-signal stability assessment for the VSI using IP controller is conducted below and the derivation of this accurate small-signal model is based on [6], which will not be shown further. There are 12 poles in total for this VSI with the PLL-based current control, and only the poles near to $x = 0$ are presented in Fig. 7(a). It is found that the VSI using the IP controller does not change the positions of these poles comparing to that of the VSI using the PI controller. Based on our proposed PI parameters for the PLL and current control, both IP and PI controllers enable the VSI to stably

connect to a very weak grid (SCR=1), as shown in Fig. 7(a). However, their performance are significantly different when a step-change is applied for the current regulation, as shown in Fig. 7(b) and (c). It is found that the IP controller stabilizes the VSI much better.

As the dominant instability mechanism of the VIS connecting to a very weak has been identified, the PLL-based PV control can be stabilized simply, which its parameters are provided below: current control: $\zeta^c = 0.707$ $w_n^c = 360$; PLL: $\zeta^{PLL} = 0.707$ $w_n^{PLL} = 120$; PV control: the power control is 10 times slower than the current control and the voltage control is 3 times faster than the power control.

The small-signal stability assessment for this PLL-based PV control is shown below. Within this PLL-based PV control, the IP controller refers to its application for the inner loop current control. There are 14 poles in total for this VSI with the PLL-based PV control, and only the poles near to $x = 0$ are presented in Fig. 8(a). Poles of this IP-based VSI control stay within the left-half plane, while two poles of the PI-based VSI control are at the right-half plane. This is indicated that this VSI using the IP controller is stabilized under the very-weak-grid condition (SCR=1), while the PI-based VSI control is unstable. The simulation validation for the above stability analysis is also presented in Fig. 8(b) and (c), it is found that this IP controller well stabilizes the VSI during its power regulation from 0 to 1 p.u.. On the contrary, the PI-based VSI control loses stability once the VSI is synchronized with the grid.

IV. CONCLUSION

The dominant instability mechanism of a VSI connecting to a very weak grid is identified, which is mainly caused by the current control. In particular, it is found k_p tuning of current PI controller cannot balance the PCC voltage impact and damping capability within such a very weak grid. This issue is solved by restructuring the PI controller as an IP controller, which effectively enables the VSI connect to a very weak grid SCR=1

with rated power injection. The conventional tuning method of current control does not change thanks to this IP controller. Our case studies were tuned in a per-unit system, which provides a general tuning experience for this stable connection including: keeping low natural frequency of current control and PLL, such as $w_n^c = 160$ and $w_n^{PLL} = 11$; enhancing damping ratio of the current control, such as $\zeta^c = 20$.

REFERENCES

[1] N. Pahalawaththa et al., "Connection of wind farms to weak ac networks," CIREG, WG B4.62, Tech. Rep., Dec. 2016.
[2] J. Rose et al., "Wind energy systems sub-synchronous oscillations: Events and modeling," IEEE Power & Energy Society, Tech. Rep., Jul. 2020.
[3] Y. Li, L. Fan, and Z. Miao, "Wind in weak grids: Low-frequency oscillations, subsynchronous oscillations, and torsional interactions," IEEE Trans. Power Syst., vol. 35, no. 1, pp. 109–118, 2020.
[4] L. Harnefors, M. Bongiorno, and S. Lundberg, "Input-admittance calculations and shaping for controlled voltage-source converters," IEEE Trans. Ind. Electron., vol. 54, no. 6, pp. 3323–3334, Dec. 2007.
[5] B. Wen, D. Boroyevich, R. Burgos, P. Mattavelli, and Z. Shen, "Analysis of d-q small-signal impedance of grid-tied inverters," IEEE Trans. Power Electron., vol. 31, no. 1, pp. 675–687, Jan. 2016.
[6] C. Li, J. Liang, L. M. Cipcigan, W. Ming, F. Colas, and X. Guillaud, "Dq impedance stability analysis for the power-controlled grid-connected inverter," IEEE Trans. Energy Convers., vol. 35, no. 4, pp. 1762–1771, Dec. 2020.
[7] Y. Li, L. Fan, and Z. Miao, "Stability control for wind in weak grids," IEEE Trans. Sustain. Energy, vol. 10, no. 4, pp. 2094–2103, 2019.
[8] J. Z. Zhou, H. Ding, S. Fan, Y. Zhang, and A. M. Gole, "Impact of short-circuit ratio and phase-locked-loop parameters on the small-signal behavior of a vsc-hvdc converter," IEEE Trans. Power Del., vol. 29, no. 5, pp. 2287–2296, Oct. 2014.
[9] A. Egea-Alvarez, S. Fekriasl, F. Hassan, and O. Gomis-Bellmunt, "Advanced vector control for voltage source converters connected to weak grids," IEEE Trans. Power Syst., vol. 30, no. 6, pp. 3072–3081, Nov. 2015.
[10] M. Davari and Y. A.-R. I. Mohamed, "Robust vector control of a very weak-grid-connected voltage-source converter considering the phase-locked loop dynamics," IEEE Trans. Power Electron., vol. 32, no. 2, pp. 977–994, Feb. 2017.
[11] M. F. M. Arani and Y. A. I. Mohamed, "Analysis and performance enhancement of vector-controlled vsc in hvdc links connected to very weak grids," IEEE Trans. Power Syst., vol. 32, no. 1, pp. 684–693, Jan. 2017.